J|A|C|S
COMMUNICATIONS

Published on Web 05/01/2007

Synthesis and Self-Assembly of fcc Phase FePt Nanorods

Min Chen,*,†,‡ Timothy Pica,† Ying-Bing Jiang,‡ Peng Li,† Kazuaki Yano,# J. Ping Liu,#
Abhaya K. Datye,† and Hongyou Fan*,†,‡

Center for Micro-Engineering Materials, University of New Mexico, New Mexico 87131, Sandia National Laboratories, Albuquerque, New Mexico 87106, and Department of Physics, University of Texas, Arlington, Texas 76019

Received December 18, 2006; Revised Manuscript Received March 23, 2007; E-mail: mchen05@unm.edu; hfan@sandia.gov

FePt nanocrystals with sizes ranging from 2 to 20 nm are an important class of magnetic nanomaterials.[1] The promising applications in data storage, high performance permanent magnets, biomedicine, and catalysis promote extensive synthetic effort. To date, most of previous work has focused on the synthesis of spherical or cubic FePt nanocrystals.[2] One-dimensional FePt nanoparticles (nanorods or nanowires) are more interesting because they are expected to have magnetic and structural anisotropy with unique magnetic properties.[1] To this end, few efforts were made on the synthesis of CoPt nanorods, CoPt nanowires, and FePt nanowires.[3] However, the resulting nanorods or nanowires were either ill-defined in shape or agglomerated, and therefore are not ideal for the formation of uniform magnetic anisotropy. Here for the first time, we report a synthesis of monodispersed FePt nanorods through confined decomposition of $Fe(CO)_5$ and reduction of $Pt(caca)_2$ in a surfactant liquid-crystal mesophase.

Transmission electron micrscopy (TEM) in Figure 1A shows the monolayer self-assembled arrays of FePt nanorods with an average diameter of 2.1 nm and a length of 11.3 nm. HRTEM images (Figure 1B,C) show FePt nanorods with both {100} and {110} faces. X-ray diffraction (XRD) pattern of the as-prepared FePt nanorods shows the strongest (111) peak at ~40.2° and a (200) peak at ~47°, (Figure 2A), corresponding to the standard face-center cubic (fcc) structure with a random crystalline orientation. Composition analysis using the energy dispersed X-ray spectroscopy EDS (Figure 2B) shows the Fe/Pt atomic ratio of ~40/60. Annealing induced the phase transformation from fcc phase to long-range chemically ordered "fct" phase, with particles sintered after annealing. Alternative gradient magnetometry (AGM) measurement on annealed FePt nanorods shows the ferromagnetism with a coercivity of ~5 kOe at room temperature (Figure 2C). We found that the uniformity of FePt nanorods was sensitive to heating rate. Reactions at a heating rate of 1 °C/min led to fairly monodisperse nanorods, while reactions at a heating rate of 10 °C/min generated a mixture of spherical and necklacelike FePt nanoparticles with an average diameter of 3 nm and a length of up to 80 nm (Figure S1).

Elemental mapping of necklacelike FePt nanoparticles on HR-TEM images shows uniform composition distribution along the *c*-axis with iron atomic percentages between 38 and 42% (Figure S2 and S3). The composition of FePt nanorods can be tuned by adjusting the molar ratio of $Fe(CO)_5/Pt(acac)_2$. The $Fe(CO)_5/Pt(acac)_2$ ratio of 2 gave $Fe_{38}Pt_{62}$ composition, as characterized by EDS. By adjusting the molar ratio of $Fe(CO)_5/Pt(acac)_2$ from 1 to 3, the atomic percentage of iron in the FePt nanorods changed from 22% to 40%. However, if the molar ratio of $Fe(CO)_5/Pt(acac)_2$ was larger than 3, spherical FePt nanocrystals began to appear in addition to nanorods. The rest of iron is in the form of Fe(II)-surfactant complex, as evidenced by the fact that the solution appeared as deep brown color after precipitation and centrifugation processes.

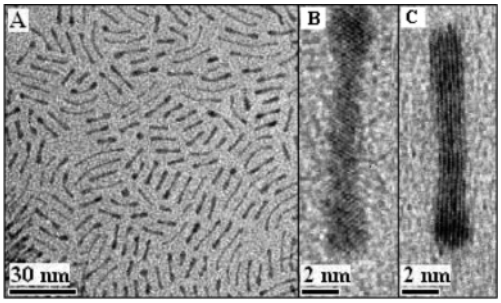

Figure 1. TEM images of FePt nanoparticles: (A) TEM images of FePt nanorods; (B) high-resolution TEM of FePt nanorods with {110} faces; (C) FePt nanorods with {100} faces.

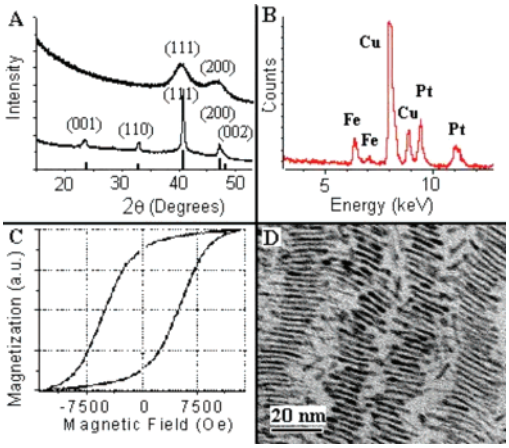

Figure 2. (A) XRD patterns of $Fe_{40}Pt_{60}$ nanorods: (top) as-prepared; (bottom) annealed under 5% H_2/95% N_2 at 700 °C for 1 h. (B) EDS of $Fe_{40}Pt_{60}$ nanorods. (C) Room-temperature magnetic hysteresis loop of the annealed $Fe_{40}Pt_{60}$ nanorods, showing a coercivity of ~5 kOe. (D) Directed-assembly of FePt nanorods under external magnetic field.

In our experiments, we found that the formation of surfactant (OA and OAm) mesophase was critical on the controlled formation of FePt nanorods. Different from the previous synthetic process in which less concentrated surfactants were used for the synthesis of spherical and cubic $FePt^{2a-c}$, we added more surfactants (OA and OAm) in the reaction solution. It is well-known that the spherical micelles of surfactants start to form in aqueous or organic solvent at a critical micelle concentration (CMC).[4] When the concentration of surfactants further increases, the shape of micelles turns from spherical to cylindrical (or rodlike), or even ordered hexagonal packing of cylindrical in organic solvents.[4] These shaped micelles have been consciously used as templates to synthesize spherical and rodlike nanocrystals.[5] In our case, highly concentrated surfac-

† University of New Mexico.
‡ Sandia National Laboratories.
# University of Texas at Arlington.

10.1021/ja069057x CCC: $37.00

tants (OA and OAm) with OAm-rich formed hexagonal reverse liquid-crystal mesophase in reaction solution, which was confirmed by the low angle XRD patterns that were conducted on specimens with and without $Pt(acac)_2$ (Figure S4 and S5). We found that addition of $Pt(acac)_2$ maintained the mesophase. This was essential because it ensured the decomposition, and the reduction reaction occurred in the confined mesophase. Reaction of hydrocarbon acid and amine slowly generates hydrocarbon amide and water. Recent report by Cao et al. confirmed the release of water from the condensation reaction between OA and OAm during nanocrystal synthesis.[6] In our reaction system, the water resulting from the condensation reaction of OA and OAm would further promote the formation of anisotropic reverse micelles to confine the decomposition of $Fe(CO)_5$ and reduction of $Pt(caca)_2$. In compared experiments, we could not get FePt nanorods in stirring condition or in an open reaction system using the same reaction solutions in which we were able to synthesize FePt nanorods in a sealed autoclave. This suggests that both the still condition and the sealed system are essential to preserve hexagonal reverse surfactant micelles for the formation of nanorods.

On the basis of the above observation, we summarized the forming process of FePt nanorods, as shown in Scheme S1. Overall, the decomposition of $Fe(CO)_5$ and reduction of $Pt(caca)_2$ was confined in the reverse cylindrical mesophase. At low heating rate, slow growth of nuclei usually occurs. This allows the FePt nanocrystals to grow continuously in the confined reverse micelles causing the formation of FePt nanorods along the reaction time course. However, at high heating rate, isotropic growth of FePt nuclei becomes dominant, which causes the formation of spherical nanocrystals at the beginning of the reaction. According to previous results, the FePt nanoparticles with spherical shape are usually produced at a high heating rate and temperature (~300 °C) reaction.[2a,b] As the precursors deplete because of the formation of FePt spheres, subsequent growth of FePt becomes slower. The confined growth of FePt along reverse micelles, then, became prevailing. Such a slow growth likely connects the spherical FePt nanoparticles and finally forms necklacelike shapes. We extended this formation process to synthesize FePt nanwires. By simply increasing the heating time from 3 to 24 h, FePt nanowires with a length up to 200 nm were able to be produced (Figure S6).

Self-assembly of FePt nanorods was conducted by evaporating a few drops of diluted FePt nanorods/hexane dispersion on silicon wafers. TEM images showed that these arrays self-assembled into ordered 3-dimensional arrays (Figure S7). By titling the TEM grid along *c*-axis for 25°, we found that some nanorods were paralleled (appeared as rod shape) and some were vertical (appeared as dot shape) to the substrate. Directed-assembly of FePt nanorods was conducted through putting the substrates between two lab magnets during formation of nanorod arrays. TEM images (Figure 2D and Figure S8) showed the nanorods were paralleled to the substrates. XRD patterns showed three Bragg reflections at 2.17°, 4.08°, and 6.05°, respectively (Figure S8). They can be indexed as (100), (200), and (300) of 2D hexagonal mesophase with unit cell $a = \sim 47$ Å, similar to the surfactant/silica mesophase reported before.[7−8] This is in good agreement with TEM images (Figure S8a).

In conclusion, we described the synthesis of FePt nanorods by confining decomposition of $Fe(CO)_5$ and reduction of $Pt(caca)_2$ in surfactants/organic solvent reverse cylindrical micelles. The controlled nucleation and growth kinetics in the confined environment allows easy control over Fe/Pt composition, nanorod uniformity, and nanorod aspect ratio. The FePt nanorods tended to self-assemble into ordered arrays along three-dimensions. Directed-assembly under external magnetic field led to 2D hexagonal ordered arrays, parallel to the substrate. We expect that with optimized external magnetic fields, we should be able to assemble these nanorods into oriented 1D or 2D arrays, providing a uniform anisotropic magnetic platform for varied applications in enhanced data storage, magneto-electron transport, etc.

Acknowledgment. This work was partially supported by the U.S. Department of Energy (DOE) Basic Energy Sciences Program, Sandia National Laboratory's Laboratory Directed R&D program, and National Science Foundation (NSF)-Sandia (Grant DMI-0625897), T.P. acknowledged the support from NSF Research Experience for Undergraduates (REU) program. TEM studies were performed in the Department of Earth and Planetary Sciences at The University of New Mexico. Sandia is a multiprogram laboratory operated by Sandia Corporation, a Lockheed Martin Company, for the U.S. DOE's National Nuclear Security Administration under Contract DE-AC04-94AL85000.

Supporting Information Available: Experimental procedure and characterization of the FePt nanorods and nanowires. This material is available free of charge via the Internet at http://pubs.acs.org.

References

(1) (a) Sun, S. *Adv. Mater.* **2006**, *18*, 393−403. (b) Zeng, H.; Li, J.; Liu, J. P.; Wang, Z. L.; Sun, S. H. *Nature* **2002**, *420*, 395−398. (c) Gu, H. W.; Ho, P. L.; Tsang, K. W. T.; Yu, C. W.; Xu, B. *Chem. Comm.* **2003**, *15*, 1966−1967. (d) Chen, W.; Kim, J.; Sun, S. H.; Chen, S. W. *Phys. Chem. Chem. Phys.* **2006**, *8*, 2779−2786. (e) Arico, A. S.; Bruce, P.; Scrosati, B.; Tarascon, J. M.; Van Schalkwijk, W. *Nat. Mater.* **2005**, *4*, 366−377.

(2) (a) Sun, S.; Murray, C. B.; Weller, D.; Folks, L.; Moser, A. Science **2000**, *287*, 1989−1992. (b) Chen, M.; Liu, J. P.; Sun, S. H. *J. Am. Chem. Soc.* **2004**, *126*, 8394−8395. (c) Chen, M.; Kim, J.; Liu, J. P.; Fan, H.; Sun, S. H. *J. Am. Chem. Soc.* **2006**, *128*, 7132−7133. (d) Elkins, K. E.; Vedantam, T. S.; Liu, J. P.; Zeng, H.; Sun, S. H.; Ding, Y.; Wang, Z. L. *Nano Lett.* **2003**, *3*, 1647−1649. (e) Liu, C.; Wu, X. W.; Klemmer, T.; Shukla, N.; Yang, X. M.; Weller, D.; Roy, A. G.; Tanase, M.; Laughlin, D. *J. Phys. Chem. B* **2004**, *108*, 6121−6123.

(3) (a) Zhang, Z. T.; Blom, D. A.; Gai, Z.; Thompson, J. R.; Shen, J.; Dai, S. *J. Am. Chem. Soc.* **2003**, *125*, 7528−7529. (b) Wang, Y.; Yang, H. *J. Am. Chem. Soc.* **2005**, *127*, 5316−5317. (c) Hou, Y. L.; Kondoh, H.; Che, R. C.; Takeguchi, M.; Ohta, T. *Small* **2006**, *2*, 235−238.

(4) Israelachvili, J. *Intermolecular and Surface Forces*; Academic: San Diego, CA, 1992.

(5) (a) Peng, X. G.; Manna, L.; Yang, W. D.; Wickhan, J.; Scher, E.; Kadavanich, A.; Alivisatos, A. P. *Nature* **2000**, *404*, 59−61. (b) Kim, F.; Song, J. H.; Yang, P. D. *J. Am. Chem. Soc* **2002**, *124*, 14316−14317. (c) Murphy, C. J.; Jana, N. R. *Adv. Mater.* **2002**, *14*, 80−82. (d) Xia, Y. N.; Yang, P. D.; Sun, Y. G.; Wu, Y. Y.; Mayers, B.; Gates, B.; Yin, Y. D.; Kim, F.; Yan, Y. Q. *Adv. Mater.* **2003**, *15*, 353−389. (e) Talapin, D. V.; Shevchenko, E. V.; Murray, C. B.; Kornowski, A.; Forster, S.; Weller, H. *J. Am. Chem. Soc.* **2004**, *126*, 12984−12988. (f) Cho, K. S.; Talapin, D. V.; Gaschler, W.; Murray, C. B. *J. Am. Chem. Soc.* **2005**, *127*, 7140−7147. (g) Gou, L. F.; Murphy, C. J. *Chem. Mater.* **2005**, *17*, 3668−3672. (h) Yin, Y.; Alivisatos, A. P. *Nature* **2005**, *7059*, 664−670.

(6) Wu, H. M.; Yang, Y. N.; Cao, Y. C. *J. Am. Chem. Soc.* **2006**, *128*, 16522−16523.

(7) Kresge, C.; Leonowicz, M.; Roth, W.; Vartuli, C.; Beck, J. *Nature* **1992**, *359*, 710−712.

(8) Yang, H.; Kuperman, A.; Coombs, N.; Mamiche-Afara, S.; Ozin, G. A. *Nature* **1996**, *379*, 703−705.

JA069057X